HHS Public Access

Author manuscript

J Neurosci Methods. Author manuscript; available in PMC 2016 April 05.

Published in final edited form as:

J Neurosci Methods. 2015 July 15; 249: 66–74. doi:10.1016/j.jneumeth.2015.04.009.

Long-term imaging of circadian locomotor rhythms of a freely crawling *C. elegans* population

Ari Winbush[a], **Matthew Gruner**[a], **Grant W. Hennig**[b], and **Alexander M. van der Linden**[a,*]

[a]Department of Biology, University of Nevada, Reno, NV 89557, USA

[b]Department of Physiology and Cell Biology, University of Nevada, School of Medicine, Reno, NV 89557, USA

Abstract

Background—Locomotor activity is used extensively as a behavioral output to study the underpinnings of circadian rhythms. Recent studies have required a populational approach for the study of circadian rhythmicity in *Caenorhabditis elegans* locomotion.

New method—We describe an imaging system for long-term automated recording and analysis of locomotion data of multiple free-crawling *C. elegans* animals on the surface of an agar plate. We devised image analysis tools for measuring specific features related to movement and shape to identify circadian patterns.

Results—We demonstrate the utility of our system by quantifying circadian locomotor rhythms in wild-type and mutant animals induced by temperature cycles. We show that 13 °C:18 °C (12:12 h) cycles are sufficient to entrain locomotor activity of wild-type animals, which persist but are rapidly damped during 13 °C free-running conditions. Animals with mutations in *tax-2*, a cyclic nucleotide-gated (CNG) ion channel, significantly reduce locomotor activity during entrainment and free-running.

Comparison with existing method(s)—Current methods for measuring circadian locomotor activity is generally restricted to recording individual swimming animals of *C. elegans*, which is a distinct form of locomotion from crawling behavior generally observed in the laboratory. Our system works well with up to 20 crawling adult animals, and allows for a detailed analysis of locomotor activity over long periods of time.

Conclusions—Our population-based approach provides a powerful tool for quantification of circadian rhythmicity of *C. elegans* locomotion, and could allow for a screening system of candidate circadian genes in this model organism.

Keywords

C. elegans; Circadian rhythms; Temperature; Locomotion; Crawling; Population

*Corresponding author. Tel.: +1 775 784 6080. avanderlinden@unr.edu (A.M. van der Linden). awinbush237@gmail.com (A. Winbush), matthew.gruner@gmail.com (M. Gruner), grant@medicine.nevada.edu (G.W. Hennig).

Appendix A. Supplementary data

Supplementary material related to this article can be found, in the online version, at http://dx.doi.org/10.1016/j.jneumeth.2015.04.009

1. Introduction

Most organisms show circadian rhythms of behavior that repeat roughly every 24 h. These rhythms are controlled by an internal clock that can be entrained by daily changes in environmental cues. In addition to light, which is considered to be the strongest zeitgeber, it has been long-known that temperature cycles can also entrain circadian rhythms. For instance, in *Drosophila*, low-amplitude temperature cycles can robustly entrain eclosion rhythms (Pittendrigh, 1954), locomotor activity rhythms (Wheeler et al., 1993; Yoshii et al., 2002), and molecular rhythms in peripheral tissues (Glaser and Stanewsky, 2005). Similar temperature cycles are able to entrain molecular rhythms and locomotory activity rhythms in zebrafish (Lahiri et al., 2005; Lopez-Olmeda et al., 2006). In mammals, natural body temperature cycles are known to keep peripheral clocks synchronized to the light cycle (Brown et al., 2002; Buhr et al., 2010). Temperature can also dominate light inputs, such as in *Neurospora* (Liu et al., 1998), and in *Drosophila* under more natural conditions (Vanin et al., 2012). Thus, although temperature cycles can reliably entrain the circadian clock in many organisms, relatively little is known about how temperature inputs control this clock.

The nematode *Caenorhabditis elegans* is an excellent system to study the neural circuits and the molecular machinery responsible for temperature-dependent responses (Garrity et al., 2011). It has a small and completely mapped nervous system, with a well-known neural circuitry that is able to sense temperature. Moreover, many genes identified in studies to be required for thermotaxic behavior, appear to play a role in temperature-sensation and processing pathways (Kimata et al., 2012). As in other animals, daily cycles of temperature can entrain circadian rhythms of *C. elegans* behavior such as locomotion (Simonetta et al., 2009) and olfaction (Olmedo et al., 2012), as well as the expression of multiple transcripts (van der Linden et al., 2010), and the oxidation state of peroxiredoxin (PRX) (Olmedo et al., 2012). In addition, several studies have reported light-entrained circadian rhythms in behavior of *C. elegans* e.g. locomotor activity (Saigusa et al., 2002; Simonetta and Golombek, 2007), defecation and pharyngeal pumping rate (Migliori et al., 2011), metabolism e.g. resistance to osmotic stress (Kippert et al., 2002), and melatonin levels (Migliori et al., 2012). Although these studies indicate that *C. elegans* has a circadian system, little remains known about the molecular and neural components of the *C. elegans* circadian clock. This may be, at least in part, due to the lack of automated methods that can robustly record and measure circadian rhythms over long periods of time at either the behavioral or molecular level.

Measuring locomotor activity rhythms of *Drosophila* and rodents has provided the main circadian output phenotype that has led to the successful identification of molecular and cellular components of the circadian clock. In *C. elegans*, locomotor activity rhythms under circadian control have also been reported. In one of these methods, individual animals swimming in single wells were video-tracked over multiple days (Saigusa et al., 2002). The other method used an infrared microbeam scattering approach similar to the *Drosophila* activity monitoring (DAM) system for *Drosophila* (TriKinetics) in which the activity of swimming animals cultured individually in 96-well micro-titer plates was recorded when animals cross an infrared light beam (Simonetta and Golombek, 2007; Simonetta et al., 2009). However, these activity rhythms of swimming animals appear to exhibit significant

animal-to-animal variability, and more than two-thirds of individual animals tested showed no clear rhythms (Simonetta and Golombek, 2007; Simonetta et al., 2009), suggesting the need for a populational approach. Moreover, swimming of *C. elegans* is a distinct form of locomotion from crawling on a standard agar surface generally used in the laboratory (Pierce-Shimomura et al., 2008).

Automated tracking systems have been developed that can analyze movement of *C. elegans* animals (Husson et al., 2012), including systems that monitor locomotor activity of either individual or multiple animals crawling on a single plate. However, although these automated tracking systems have greatly improved ways of detecting and characterizing locomotor behavior of animals during short periods of time (hours), they are limited in recording and analyzing long-term circadian rhythms (days, or even weeks). For instance, the parallel worm tracker software widely used by many labs extracts movement features of multiple crawling animals simultaneously (such as speed and travel path) from uncompressed video files (Ramot et al., 2008a,b). This method limits the amount of time videos can be recorded, and it would be impractical when multi-day video recordings are necessary for each circadian experiment. Similarly, the multi-worm tracker software is designed to extract movement features of multiple animals simultaneously, but in real-time at high-speed and high-resolution (Swierczek et al., 2011). Although this method provides a rapid and more accurate quantification of movement when behavior changes over minutes or even hours, this real-time feature is not particularly useful for long term recording of circadian rhythms (Winbush and van der Linden, pers. comm.). Furthermore, the multi-worm tracking system requires additional expensive software from National Instruments (Swierczek et al., 2011). More recently, the multi-well imaging technique has been reported as a method for long-term imaging of locomotor activity throughout development (from L1 to adults) such as behavioral quiescence (Yu et al., 2014). However, the custom analysis software used in this multi-well imaging method is limited to extracting movement of individual animals with each crawling in a separate agar-filled well.

We therefore designed a new imaging method that is easy to implement, inexpensive and enables the long-term automated recording and analysis of locomotor activity of *C. elegans* needed for circadian studies. In our method, we devised new image analysis tools to extract movement (i.e. activity, trajectories, body bends) and shape (i.e. body length) features from videos recorded over several days of multiple animals crawling on the surface of an agar plate. Using this population approach, we were able to obtain measurements of circadian locomotor activity of wild-type and mutant animals of *C. elegans* induced by temperature cycles.

2. Material and methods

2.1. C. elegans culture and entrainment conditions

We used a N2 Bristol wild-type strain provided by the *Caenorhabditis* Genetic Center (CGC). Animals were synchronized to the same developmental stage by the hypochlorite method and cultured on Nematode Growth Media (NGM) agar seeded with a lawn of *E. coli* OP50 as the primary food source. Growth-synchronized populations of L1 larvae were entrained to 18 °C:13 °C temperature cycles until either the L4 stage or the young adult

stage (approximately 3 or 4 days post L1 larval stage, respectively). About 5–20 young adult animals were then transferred onto a 5-cm assay plate freshly seeded with a thin circular layer of *E. coli* OP50 (100 μl). The assay plate contained a low concentration of peptone (50% of normal) in order to minimize growth and thickness of the bacterial lawn, and 50 μM 5-fluoro-2-deoxyuridine (FUDR) to prevent self-reproduction (Mitchell et al., 1979). This concentration of FUDR dramatically reduced the growth of any new progeny produced by the parents when they were transferred onto the FUDR plate as either L4 larvae or young adults, and did not interfere with the tracking of the parents. Of note, transfer of L4 animals to FUDR-containing plates gives a better circadian character. The circular diameter of the OP50 bacterial lawn was kept at 2-cm in order to keep worms within the field of view (FOV) of the camera (see below). After the transfer, animals on the assay plates were continuously entrained by temperature cycles of 13 °C:18 °C (12:12 h) in constant darkness (DD) followed by constant free-running conditions at 13 °C (unless indicated otherwise). The transfer of animals onto a plate and placing it in the imaging system was done during the warm phase under red light illumination. Red light does not appear to have an effect on circadian activity of swimming *C. elegans* (Simonetta et al., 2009). All experiments were performed in programmable temperature- and light controlled incubators (Percival Scientific, model I-36VL). Temperature stability in the incubator chamber and proper cycling were verified through the use of an infrared temperature sensor (Omega Engineering Inc., Stamford CT, IR-USB) aimed directly at the assay plate during temperature cycles and free-running conditions.

2.2. Imaging system for circadian experiments

The imaging set-up consisted of a digital camera, a lens, a red light LED illuminator, and mechanical parts (Fig. 1A). We used either a USB 2.0 or FireWire monochrome camera (Point Grey Research, CMLN-13S2M-CS or GS2-FW-14S5M, respectively) with either a 12.5 mm or 25 mm focal length C-mount lens (Fujinon, HF12.5HA-1B or HF25HA-1B, respectively). Cameras were attached to a 1.5 in. diameter mounting post (Thorlabs, P10) via a 2.5 in. post-clamp (Thorlabs, C1501), and the whole assembly was attached to a large aluminum breadboard (Thorlabs, PBG series). Assay plates (5 cm diameter) were placed on a small stage consisting of a small aluminum breadboard, attached to the larger breadboard with 1 in. diameter pillar post (Thorlabs, RS series). To minimize vibration from the incubator, each breadboard assembly was placed on a 0.5 in. thick Sorbothane pad. Animals on the assay plate were illuminated using a low-angle red light LED ring with an inner diameter of 110 mm and light wavelength of 630 nm (CCS America Inc., LDR-146RD2-LA1), powered by a 24 V power supply (CCS America Inc., PD2-1024). This dark field illumination showed animals as white objects against a relatively dark background.

2.3. Video recording

Video images were captured with FlyCapture SDK software (Point Grey Research) installed on a Dell XPS Windows 7 desktop. Camera input was set at one frame per second (FPS), and one out of every 3 or 5 frames (0.33/0.2 FPS) was saved to the disk for further analysis. Combined with dark field illumination, this enabled us to record non-stop videos for up to 96 h in compressed AVI format (Fig. 1B). Videos were then converted into QuickTime (H.

264) movie format. The field of view (FOV) of most movies was ~22 mm^2 (464 × 440 pixels) captured at a rate of one frame every 3 or 5 s (0.33/0.2 FPS).

2.4. Image analysis and worm tracking for circadian experiments

After completion of video conversion, we imported the QuickTime movies into Volumetry software (Hennig et al., 1999), which is an off-line custom-developed "sandbox" application to write and execute code for 1D-4D image analysis that runs on the Macintosh OS X operating system. Movies were decompressed to stacks of 8-bit grayscale images subdivided into 3GB sections (~10,000 frames). To detect and track worms from these movies, we designed the following image processing steps in the Volumetry environment (Fig. 2A and B): (1) initial intensity threshold to outline animals sufficiently to perform an average static background subtraction; (2) the application of a 3 × 3 pixel Gaussian kernel filter (s.d. 1.0); (3) the application of an intensity threshold to outline animals adequately (same threshold for all subsections); and (4) the blacking out of threshold particles that were less than 0.13 mm^2 (50 pixels). The Gaussian filtering slightly inflated the width and shortened the length of worms (by ~1 pixel), but was necessary to allow automated particle analysis free from sub-artifacts and particles too thin to analyze (overall area change <10%). When necessary, custom-build software allowed for concatenation of videos into a single movie sequence of frames for analysis with an elapsed time of 1 s between videos.

2.4.1. Detection of worms by creating particle files—Storing the shape and position of animals as conventional bitmaps was inefficient as the area of animals was <1% of the FOV. Instead, each frame was scanned for pixels within the intensity threshold, and if detected, the full extent of the animal was flood-filled. The following information was then stored per frame: (1) arbitrary animal number (in order of appearance from top → bottom of frame); (2) size (in pixels); (3) minimum X and Y position from each animals' bounding rectangle; and (4) particle coordinates in relation to the minimum X and Y position (8-bit). This reduced the file size from ~2GB per 10 K frames to 10–20Mb depending on the number of animals in the FOV (n = 5–20). The individual particles files from the 10 K frame subsections were then concatenated together into one file.

2.4.2. Tracking of worms—Upon loading a particle file, the centroid position, X and Y coordinates and bounding rectangle for each animal at each time-point was loaded and/or calculated. As the acquisition frame rate was comparatively high (0.2–0.33 Hz) a frame-by-frame particle overlap tracking routine was used (the maximum velocity of animals never exceeded 0.5 mm s^{-1}) that was more accurate than centroid tracking routines (i.e. location of a particle centroid in the next frame within a given radius tolerance). A size threshold was applied that excluded overlapping animals from the analysis (~130% of largest animal area). The particle overlap tracking method involved using the area of an animal from the previous time-point and calculation of the number of overlapping coordinates in the current frame. The trajectory of each animal that was successfully tracked for at least 30 s was given a unique positive identifying number, replacing the original arbitrary ID. Animals that could not be tracked for at least 30 s were given a negative identifying number.

2.4.3. Extracting features of locomotion and shape from images—We developed analytical tools in the Volumetry environment to extract a wide range of features related to movement and shape from the particle-based analysis approach (Fig. 1C). First, to detect overall movement, we calculated the instantaneous velocity or iVel (μm s^{-1}) by comparing the centroid position of each animal in adjacent frames. The absolute (no negative values) iVel was calculated, which did not discriminate between longitudinal or side-to-side movements, nor forward or backward movements of animals. However, this iVel calculation was useful to give an overall indication of the degree of displacement of an animal over time. Second, the endpoints of each animal were located by: first, finding the particle coordinate the furthest from the centroid position (Endpoint Maximum, or EM; Fig. 2C), then finding the particle coordinate that was furthest from the centroid in the opposite direction of the centroid–EM angle (>±60° of centroid–EM angle: Endpoint Opposite, or EO; Fig. 2C). The following parameters were calculated and stored for every successfully tracked animal at every time-point with Δ indicating the change in a parameter between adjacent time-points: (1) Area and Δ Area (μm^2); (2) orientation angle and linearity using regression analysis (° and R^2, respectively: + Δ° and ΔR^2); (3) length (centroid-to-EM + centroid-to-EO, μm: + Δ length); (4) kink-angle (centroid-to-EM° − EO-to-centroid°: + Δ kink-angle); and (5) instantaneous velocity (iVel μm s^{-1}) (Fig. 2C).

Spatio-temporal maps were developed that displayed parameters of shape or locomotion without the need to average or otherwise compress data. Briefly, the maximum number of successfully tracked animals was calculated for each experiment and an equivalent number of slots created in an image. The width of these slots allowed pixels time-points to be stacked vertically for a given overall horizontal solution. Each pixel, representing a parameter at a given time-point for a given animal, was color-coded according to magnitude of the parameter being displayed. Where appropriate, density slicing and/or thresholding was used to better display the temporal distribution of parameters within a certain magnitude range. Combining two or more parameters (within set ranges) to define a particular shape or behavioral state was utilized. Protocols and software tools for detection, tracking and extraction of features related to shape and locomotion can be made publically available and upon request.

2.5. Circadian analysis

Text output files of any of the calculated parameters can be saved and used for further analysis of circadian patterns in locomotion. We employed methods of autocorrelation and spectral analysis (MESA) to assess rhythmicity and estimate the period as described previously (Levine et al., 2002). For analysis of free-running data, we employed both the Lomb–Scargle periodogram analysis with help of the Image J plug-in called ActogramJ (Schmid et al., 2011), and sine-curve fitting using Circwave software (by R. Hut, available at www.euclock.org).

To analyze anticipatory behavior, raw data was binned in 10 min average intervals and an “anticipation index” to the warm phases was calculated by determining the fraction of total activity spanning 3 h before the warm phase transition relative to total activity spanning 6 h before the transition as previously described (Harrisingh et al., 2007). For calculating “phase

differences", the onset of increased activity was determined using ActogramJ (Schmid et al., 2011) and was defined as the time point at which the average iVel exceeded the median value for all smoothed data points across the entire period.

3. Results and discussion

3.1. Locomotor activity rhythms of a free-crawling C. elegans population are entrained by temperature cycles

To capture circadian rhythms in locomotor activity of a freely-crawling *C. elegans* population entrained by temperature cycles, we decided to use cycles between 13 °C and 18 °C. This entrainment protocol is comparable to other previously reported protocols (Supplemental Table 1), and has a similarly low temperature range (13 °C:16 °C) used to robustly measure circadian rhythmicity in olfactory behavior (Olmedo et al., 2012), which does not affect viability (Olmedo and Merrow, pers. comm.). Furthermore, given the diverse locations from which nematodes including *C. elegans* have been isolated in the wild above ground, such as in different types of rotting plant material (e.g. fruits, stems and flowers), or when dispersed through invertebrate carriers (e.g. snails) (Félix and Braendle, 2010), it is likely that such nematodes are routinely exposed to high-amplitude temperature cycles similar to our entrainment protocol (13 °C:18 °C).

When the free-crawling population was entrained to temperature cycles of 13 °C:18 °C (12:12 h) under constant dark conditions (DD) (see Section 2), we found that animals exhibited an increased locomotor activity (represented as the average instantaneous velocity, iVel in μm s^{-1}) during the warm (18 °C) phase compared to the cold (13 °C) phase (Fig. 3A). We calculated circadian parameters for the population of animals during 13 °C:18 °C temperature cycles by applying an autocorrelation and spectral analysis (MESA) on raw locomotor data (Levine et al., 2002), and found an averaged period length of 24.2 h for locomotor activity (iVel) (Supplemental Figure 1A). We note that the increased locomotor activity (iVel) of crawling animals during the warm (18 °C) phase is consistent with previous reports of swimming activity of individual *C. elegans* conducted with low-amplitude temperature cycles (Simonetta et al., 2009).

To further refine extraction of features related to movement and shape of *C. elegans* during 13 °C:18 °C temperature cycles, we determined the instantaneous velocity (iVel), body length (μm), and body bends (linearity depicted as the R^2 value) of individual animals on the assay plate that can be successfully tracked for about 30 s, and generated spatio-temporal maps with each lane corresponding to individual animals being tracked at any given instant (Fig. 3B–D). This spatio-temporal map analysis validates our results that during the cold (13 °C) phase individual animals are slow moving and exhibit higher incidents of decreased body bends (high R^2 value, Fig. 3D) compared to the warm (18 °C) phase. These incidents of decreased body bends inversely correlate with increased body length as measured with endpoint analysis (Fig. 3C) and is consistent with periods of decreased locomotor activity (Fig. 3B). We also observed that animals exhibited transient bursts of frenetic locomotor activity (high-amplitude averaged iVel) coinciding in a warm onset during cold-to-warm (13–18 °C) transitions (Fig. 3A; Supplemental Movie 1). Interestingly, this sudden increase in locomotor activity mimics a startle response observed during entrainment to light/dark

cycles in *Drosophila* when lights are turned on and off (Wheeler et al., 1993), which reflects a masking effect produced by light (Mrosovsky, 1999). Similarly, the high-amplitude activity levels (startle response) we observe is likely a component of masking when temperature increases during the cold-to-warm transition.

To further examine how animals behave during this startle response, we visualized the trajectories of each animal during a cold-to-warm (13–18 °C) transition. A 3-dimensional "spaghetti plot" of individual animal trajectories on the bacterial lawn plotted against time revealed a dramatic increase in individual instantaneous velocity (iVel) immediately after the temperature transition to the warm (18 °C) phase followed by a subsequent decrease to more stable but elevated activity levels compared to the cold (13 °C) phase (Supplemental Movie 2). Larger numbers of adult animals (>20) significantly increased the number of collisions, causing trajectories of animals to be lost more quickly (data not shown), and thus we decided to video record between 5 and 10 animals during our circadian experiments.

3.2. Locomotor activity rhythms of a free-crawling C. elegans population show anticipatory behavior to the warm phase

To determine whether temperature cycles was indeed entraining and not masking, we decided to change the structure of the temperature period in *C. elegans* similar as previously described in *C. elegans* and yeast (Olmedo et al., 2012; Eelderink-Chen et al., 2010). If locomotor activity rhythms of crawling adult animals are entrained, then we would expect to observe anticipation of the warm phase when changing the temperature period by pushing back the warm phase by 6 h (18:6 h cycle). We therefore performed an independent experiment by submitting animals to 13 °C:18 °C (12:12 h) cycles followed by a 13 °C: 18 °C (18:6 h) cycle on the last day (Fig. 4A). As expected, delaying the onset of the warm phase by 6 h caused a corresponding anticipation of locomotor activity (iVel) relative to the temperature cycle with a 6.1 h phase difference (Fig. 4B; see Section 2). In addition, we measured the anticipation index for each 12:12 h entrainment day (Fig. 4C; Harrisingh et al., 2007), and found that wild-type animals exhibit an anticipatory increase in locomotor activity (iVel) preceding the warm-onset (an average anticipation index of 0.58 calculated for 3 days).

Taken together, these results suggest that increased locomotor activity (iVel) levels can be dissected into two components: a low-amplitude anticipatory component that steadily increases several hours before the warm-onset suggesting entrainment, and a much larger high-amplitude startle response component during a cold-to-warm transition indicating the increase in temperature itself induces a masking effect.

3.3. Locomotor activity rhythms of a free-crawling C. elegans population are maintained in constant conditions but are rapidly damped

To reveal the circadian property called free-running whereby daily locomotor rhythms persist in the absence of temperature cycles (Pittendrigh, 1960), we performed an independent experiment in which the free-crawling population was released into constant cold (13 °C) conditions (12:12 h in DD) following entrainment by 13 °C:18 °C temperature cycles. We found that in free-running conditions the average locomotor activity (iVel) is

increased during subjective warm phase and persists for at least 1 day, but locomotor rhythms dampen quickly afterwards (Fig. 5A and C). The phenomenon of damping (e.g. rhythms with gradually decreasing amplitude that without environmental input vanish within a few days) has been shown previously in other organisms, such as in the yeast *Saccharomyces cerevisiae* (Eelderink-Chen et al., 2010) and in peripheral *Drosophila* rhythms (Hardin, 1994). Because we were limited to analyzing one free-running day, we used the Lomb–Scargle periodogram (ActogramJ) and sine-wave fitting software (Circwave) to determine periodicity, which resulted in a 23.8 and 25.1 h period ($P < 0.05$), respectively (Supplemental Figure 1B). Interestingly, the high-amplitude startle response component persists during entrainment days, but disappears immediately upon release into constant conditions (Fig. 5A). Taken together, our results of temperature entrainment and free-running suggests that the circadian system of a freely-crawling *C. elegans* population exhibits properties of a weak, damped oscillator, at least under the conditions used in our experiments.

3.4. Loss of tax-2 alters locomotor activity during temperature entrainment

We next examined whether our imaging method could be used to detect changes in locomotor activity rhythms of mutant strains entrained by temperature cycles when compared to wild-type animals. We focused on the cyclic nucleotide-gated (CNG) ion channel, *tax-2* in *C. elegans*, which is expressed in the primary AFD thermosensory neuron type and plays an important role in thermotaxic behavior in *C. elegans* (Hedgecock and Russell, 1975; Coburn and Bargmann, 1996). Moreover, *tax-2* mutants are known to eliminate both cooling- and warming-activated thermoreceptor currents in AFD neurons, suggesting that *tax-2* is required for thermotransduction (Ramot et al., 2008a,b). Compared to wild-type animals (Fig. 5A), we found that the increased average locomotor activity (iVel) rhythms during the warm (18 °C) phase is significantly reduced in loss-of-function *tax-2(p671)* mutant animals in both entrainment and free-running conditions (Fig. 5B and C). It is possible that *tax-2* mutants are less active compared to wild-type animals, however, *tax-2* animals do not appear to show overall movement defects (Yamada and Ohshima, 2003). Analysis of periodicity with the Lomb–Scargle method showed no clear free-running activity component in *tax-2* mutant animals that is close to 24 h (Supplemental Figure 1B). Interestingly, the startle response is still present during a cold-to-warm transition, albeit with reduced amplitude (Fig. 5B). Taken together, consistent with our previous findings (van der Linden et al., 2010), these results suggest that *tax-2* is likely required to transduce the temperature zeitgeber to the *C. elegans* circadian clock.

4. Conclusions

In summary, our imaging system constitutes the first accessible and comprehensive method to track a population of free-crawling *C. elegans* over long periods of time that allows the analysis of circadian rhythms of locomotion. Our experiments of wild-type animals show that this method results in robust entrainment of locomotor activity rhythms, although these rhythms dampen rapidly in constant free-running conditions. Since various genes and neurons required for temperature-sensation and processing pathways as well as *C. elegans* clock homologs have been described, this method now allows for a candidate approach to

screen for disruptions of circadian locomotor activity rhythms in genetic mutants, and strains in which temperature-sensing neurons have been genetically ablated. As proof of principle, we found that mutants of the cyclic nucleotide-gated (CNG) channel, *tax-2*, significantly altered locomotor activity rhythms during entrainment and free-running. Thus, our system is a new powerful tool for studying the *C. elegans* clock that may advance our efforts toward understanding how temperature controls the circadian clock. In addition, our system and software tools could be used for the examination of natural populations of *C. elegans*, especially those that vary in their temperature preferences and fitness, which may inform us about the basis of circadian behavioral traits in nature. Although this study focused on the circadian rhythmic analysis of *C. elegans* locomotion, our method also allows the analysis of other behavioral phenotypes over extended periods of time, such as adult behavioral quiescence. Moreover, experiments described here use an inexpensive imaging set-up and easy to use software tools that can be readily used for long-term video recording and analysis of behavior in any other similarly small animal.

Supplementary Material

Refer to Web version on PubMed Central for supplementary material.

Acknowledgements

We like to thank Martha Merrow for discussions and comments on the manuscript. We also would like to thank Joel Levine and Harold Dowse for providing us with analytical tools for the measurement of circadian patterns. We are grateful to the *Caenorhabditis* Genetics Center (CGC) for the wild-type and *tax-2* mutant strain used in this study. This work was supported by the National Institute of General Medical Sciences P20GM103650 (AML) and P20GM103513 (GWH), the National Institute of Neurological Disorders and Stroke R21NS078617 (AML), and the National Center for Research Resources P20RR018751 (GWH) from the National Institutes of Health.

References

Brown SA, Zumbrunn G, Fleury-Olela F, Preitner N, Schibler U. Rhythms of mammalian body temperature can sustain peripheral circadian clocks. Curr Biol. 2002; 12:1574–83. [PubMed: 12372249]

Buhr ED, Yoo SH, Takahashi JS. Temperature as a universal resetting cue for mammalian circadian oscillators. Science. 2010; 330:379–85. [PubMed: 20947768]

Coburn CM, Bargmann CI. A putative cyclic nucleotide-gated channel is required for sensory development and function in *C. elegans*. Neuron. 1996; 17:695–706. [PubMed: 8893026]

Eelderink-Chen Z, Mazzotta G, Sturre M, Bosman J, Roenneberg T, Merrow M. A circadian clock in *Saccharomyces cerevisiae*. Proc Natl Acad Sci U S A. 2010; 107:2043–7. [PubMed: 20133849]

Félix MA, Braendle C. The natural history of Caenorhabditis elegans. Curr Biol. 2010; 20(22):R965–9. [PubMed: 21093785]

Garrity PA, Goodman MB, Samuel AD, Sengupta P. Running hot and cold: behavioral strategies, neural circuits, and the molecular machinery for thermotaxis in *C. elegans* and *Drosophila*. Genes Dev. 2011; 24:2365–82. [PubMed: 21041406]

Glaser FT, Stanewsky R. Temperature synchronization of the *Drosophila* circadian clock. Curr Biol. 2005; 15:1352–63. [PubMed: 16085487]

Hardin PE. Analysis of period mRNA cycling in *Drosophila* head and body tissues indicates that body oscillators behave differently from head oscillators. Mol Cell Biol. 1994; 14:7211–8. [PubMed: 7935436]

Harrisingh MC, Wu Y, Lnenicka GA, Nitabach MN. Intracellular Ca2+ regulates free-running circadian clock oscillation *in vivo*. J Neurosci. 2007; 27:12489–99. [PubMed: 18003827]

Hedgecock EM, Russell RL. Normal and mutant thermotaxis in the nematode *Caenorhabditis elegans*. Proc Natl Acad Sci U S A. 1975; 72:4061–5. [PubMed: 1060088]

Hennig GW, Costa M, Chen BN, Brookes SJ. Quantitative analysis of peristalsis in the guinea-pig small intestine using spatio-temporal maps. J Physiol. 1999; 517(Pt 2):575–90. [PubMed: 10332103]

Husson SJ, Costa WS, Schmitt C, Gottschalk A. Keeping track of worm trackers. WormBook: The Online Review of *C. elegans* Biology. 2012:1–17.

Kimata T, Sasakura H, Ohnishi N, Nishio N, Mori I. Thermotaxis of *C. elegans* as a model for temperature perception, neural information processing and neural plasticity. Worm. 2012; 1:31–41. [PubMed: 24058821]

Kippert F, Saunders DS, Blaxter ML. *Caenorhabditis elegans* has a circadian clock. Curr Biol. 2002; 12:R47–9. [PubMed: 11818076]

Lahiri K, Vallone D, Gondi SB, Santoriello C, Dickmeis T, Foulkes NS. Temperature regulates transcription in the zebrafish circadian clock. PLoS Biol. 2005; 3:e351. [PubMed: 16176122]

Levine JD, Funes P, Dowse HB, Hall JC. Signal analysis of behavioral and molecular cycles. BMC Neurosci. 2002; 3:1. [PubMed: 11825337]

Liu Y, Merrow M, Loros JJ, Dunlap JC. How temperature changes reset a circadian oscillator. Science. 1998; 281:825–9. [PubMed: 9694654]

Lopez-Olmeda JF, Madrid JA, Sanchez-Vazquez FJ. Light and temperature cycles as zeitgebers of zebrafish (*Danio rerio*) circadian activity rhythms. Chronobiol Int. 2006; 23:537–50. [PubMed: 16753940]

Migliori ML, Romanowski A, Simonetta SH, Valdez D, Guido M, Golombek DA. Daily variation in melatonin synthesis and arylalkylamine N-acetyltransferase activity in the nematode *Caenorhabditis elegans*. J Pineal Res. 2012; 53:38–46. [PubMed: 21995323]

Migliori ML, Simonetta SH, Romanowski A, Golombek DA. Circadian rhythms in metabolic variables in *Caenorhabditis elegans*. Physiol Behav. 2011; 103:315–20. [PubMed: 21315097]

Mitchell DH, Stiles JW, Santelli J, Sanadi DR. Synchronous growth and aging of *Caenorhabditis elegans* in the presence of fluorodeoxyuridine. J Gerontol. 1979; 34:28–36. [PubMed: 153363]

Mrosovsky N. Masking: history, definitions, and measurements. Chronobiol Int. 1999; 16:415–29. [PubMed: 10442236]

Olmedo M, O'Neill JS, Edgar RS, Valekunja UK, Reddy AB, Merrow M. Circadian regulation of olfaction and an evolutionarily conserved, nontranscriptional marker in *Caenorhabditis elegans*. Proc Natl Acad Sci U S A. 2012; 109:20479–84. [PubMed: 23185015]

Pierce-Shimomura JT, Chen BL, Mun JJ, Ho R, Sarkis R, McIntire SL. Genetic analysis of crawling and swimming locomotory patterns in *C. elegans*. Proc Natl Acad Sci U S A. 2008; 105:20982–7. [PubMed: 19074276]

Pittendrigh CS. On temperature independence in the clock system controlling emergence time in *Drosophila*. Proc Natl Acad Sci U S A. 1954; 40:1018–29. [PubMed: 16589583]

Pittendrigh CS. Circadian rhythms and the circadian organization of living systems. Cold Spring Harb Symp Quant Biol. 1960; 25:159–84. [PubMed: 13736116]

Ramot D, Johnson BE, Berry TL, Carnell L, Goodman MB. The Parallel Worm Tracker: a platform for measuring average speed and drug-induced paralysis in nematodes. PLoS ONE. 2008a; 3(5):e2208. [PubMed: 18493300]

Ramot D, MacInnis BL, Goodman MB. Bidirectional temperature-sensing by a single thermosensory neuron in *C. elegans*. Nat Neurosci. 2008b; 11(8):908–15. [PubMed: 18660808]

Saigusa T, Ishizaki S, Watabiki S, Ishii N, Tanakadate A, Tamai Y, et al. Circadian behavioural rhythm in *Caenorhabditis elegans*. Curr Biol. 2002; 12:R46–7. [PubMed: 11818075]

Schmid B, Helfrich-Förster C, Yoshii T. A new Image J plug-in "ActogramJ" for chronobiological analyses. J Biol Rhythms. 2011; 26(5):464–7. [PubMed: 21921300]

Simonetta SH, Golombek DA. An automated tracking system for *Caenorhabditis elegans* locomotor behavior and circadian studies application. J Neurosci Methods. 2007; 161:273–80. [PubMed: 17207862]

Simonetta SH, Migliori ML, Romanowski A, Golombek DA. Timing of locomotor activity circadian rhythms in *Caenorhabditis elegans*. PLoS ONE. 2009; 4:e7571. [PubMed: 19859568]

Swierczek NA, Giles AC, Rankin CH, Kerr RA. High-throughput behavioral analysis in *C. elegans*. Nat Methods. 2011; 8:592–8. [PubMed: 21642964]

van der Linden AM, Beverly M, Kadener S, Rodriguez J, Wasserman S, Rosbash M, et al. Genome-wide analysis of light- and temperature-entrained circadian transcripts in *Caenorhabditis elegans*. PLoS Biol. 2010; 8:e1000503. [PubMed: 20967231]

Vanin S, Bhutani S, Montelli S, Menegazzi P, Green EW, Pegoraro M, et al. Unexpected features of *Drosophila* circadian behavioural rhythms under natural conditions. Nature. 2012; 484:371–5. [PubMed: 22495312]

Wheeler DA, Hamblen-Coyle MJ, Dushay MS, Hall JC. Behavior in light-dark cycles of *Drosophila* mutants that are arrhythmic, blind, or both. J Biol Rhythms. 1993; 8:67–94. [PubMed: 8490212]

Yamada Y, Ohshima Y. Distribution and movement of *Caenorhabditis elegans* on a thermal gradient. J Exp Biol. 2003; 206:2581–93. [PubMed: 12819265]

Yoshii T, Sakamoto M, Tomioka K. A temperature-dependent timing mechanism is involved in the circadian system that drives locomotor rhythms in the fruit fly *Drosophila melanogaster*. Zool Sci. 2002; 19:841–50. [PubMed: 12193800]

Yu CC, Raizen DM, Fang-Yen C. Multi-well imaging of development and behavior in Caenorhabditis elegans. J Neurosci Methods. 2014; 223:35–9. [PubMed: 24321627]

HIGHLIGHTS

- We describe a new system for long-term recording of circadian locomotor rhythms.
- We measured locomotor activity of a population of freely crawling adult animals.
- Novel analysis tools are used to quantify features related to movement and shape.
- Our method is simple and broadly useful for tracking of *C. elegans* phenotypes.

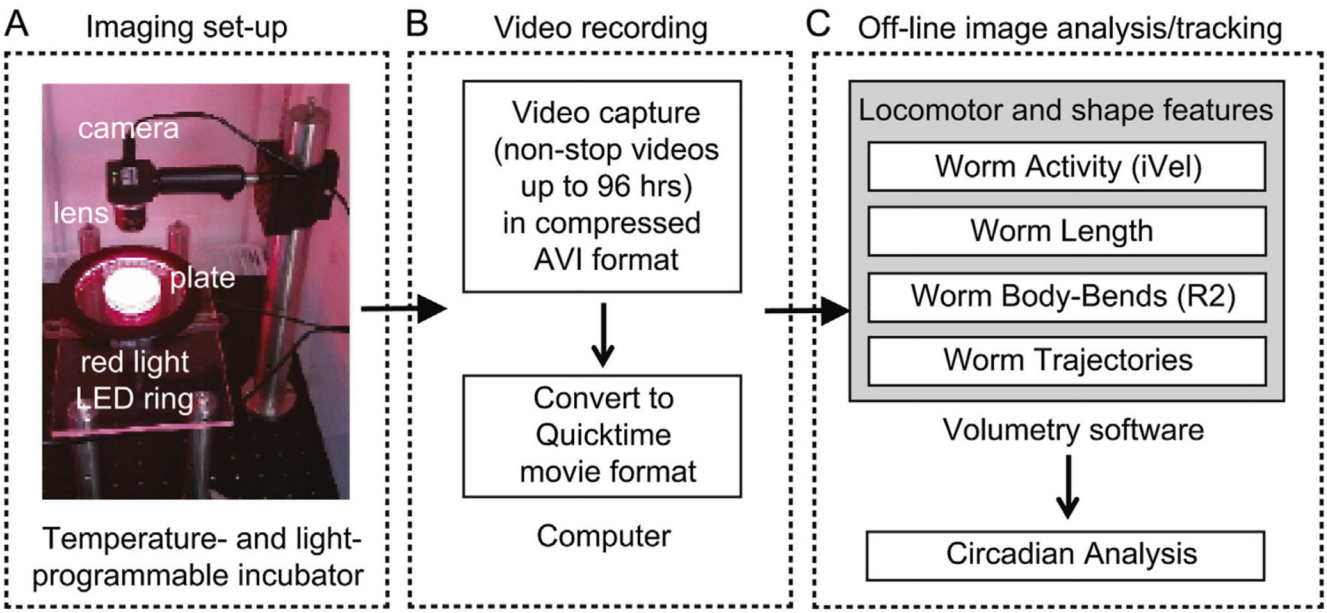

Fig. 1.

Three-step process for circadian analysis of locomotion data entrained by temperature cycles. (A) Photograph of the imaging set-up. A monochrome digital camera with lens is placed inside a temperature- and light controlled incubator and outputs video images (1 image per 3–5 s, 30–40 μm/pixel) of multiple animals moving on the surface of a single agar plate to a computer. A red light LED source is used for dark-field illumination of animals. (B) Video images of moving animals within the population are captured (1 frame every 3–5 s) and converted into a single QuickTime movie file. (C) Movies are imported into an off-line custom written image analysis software within the Volumetry application environment, which computes and extracts measurements of locomotion (instantaneous velocity, or iVel in $\mu m\ s^{-1}$), shape (worm length in μm; the R^2 value for linearity (degree of body bends)), and individual trajectories of each adult animal within the population from images. Once completed, text files are automatically created with a matrix of locomotion data versus time for each animal (e.g. activity, position, shape, trajectories), which subsequently can be used for graphical output and circadian analysis. (For interpretation of the references to color in this figure legend, the reader is referred to the web version of this article.)

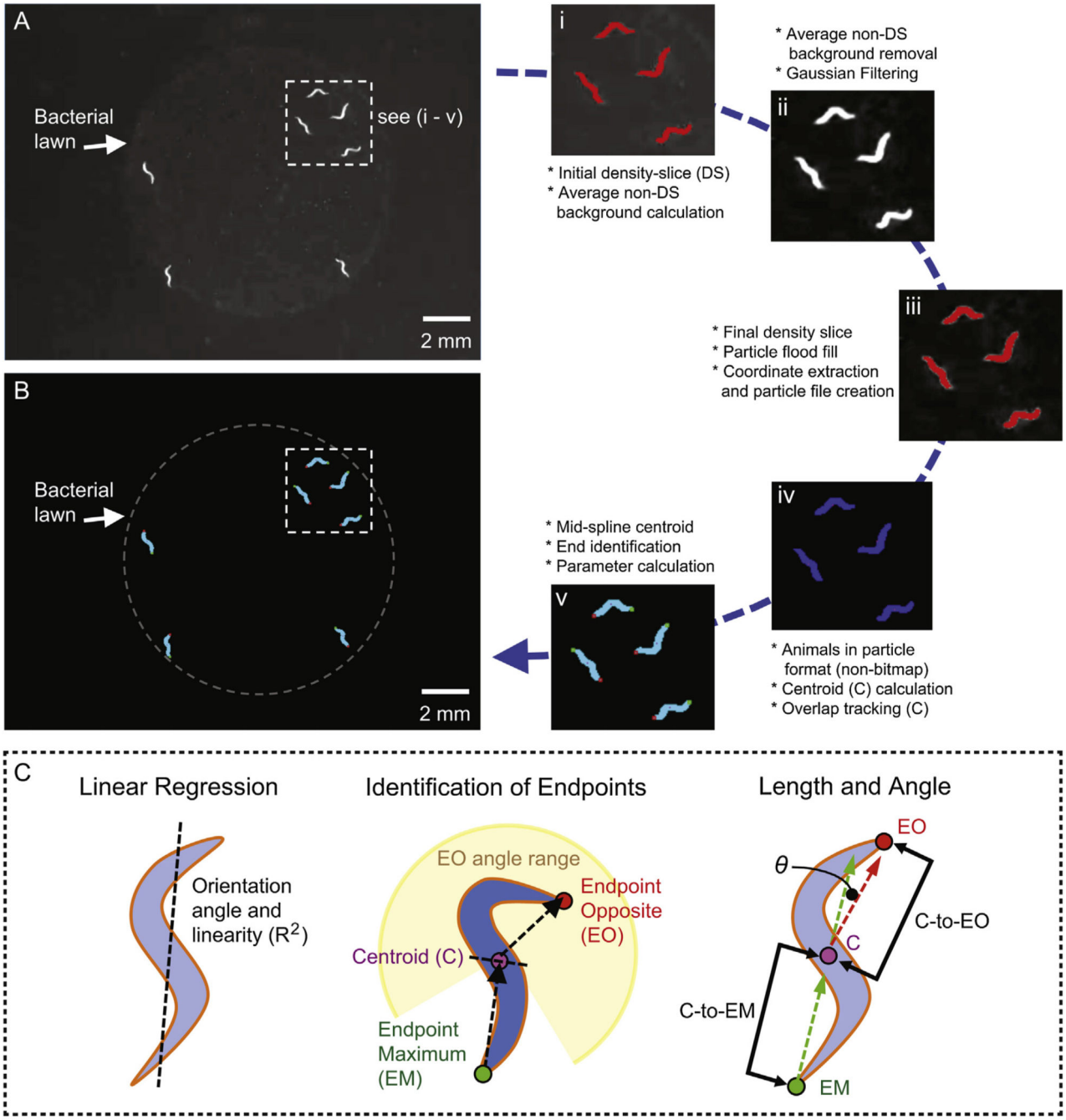

Fig. 2.

General overview of acquisition and processing of image data. Shown is a gray scale raw image of multiple animals acquired by the imaging system. Animals are easily recognized as light objects on dark backgrounds by dark-field illumination. The inset (3.5 × 3.5 mm) depicts sequential image processing steps (i–v) from the original raw image (A) to the final image (B) as described in Section 2. (C) Schematic of the orientation angle and linear regression analysis (left), the centroid and endpoint detection (middle), and length and kink angle determination (right). Briefly, we designed the following rundown analysis: (1)

Overall angle of the animal by linear regression (−90 to +90, with 0° = 12 o'clock); (2) animal copied and rotated to +90° and linear regression recalculated to get Pearson's R^2 value (i.e. how "straight" the animal is). The rotation maximizes the number of χ steps; (3) the endpoint maximum (EM) (green) coordinate furthest from the centroid (C) position (purple); (4) the centroid (C) is relocated laterally into the middle of the animal based on the perpendicular angle between the endpoint maximum (EM) coordinate and the original centroid (C); (5) the endpoint opposite (EO) (red) particle coordinate furthest from the centroid in the opposite direction of the centroid–EM angle; (6) parameters calculated from a single frame include: "Kink" angle (Δ angle between EM-to-C, and C-to-OE); and "Length" (additive distance between C-to-EM, and C-to-OE). A more detailed analysis is described in Section 2. (For interpretation of the references to color in this figure legend, the reader is referred to the web version of this article.)

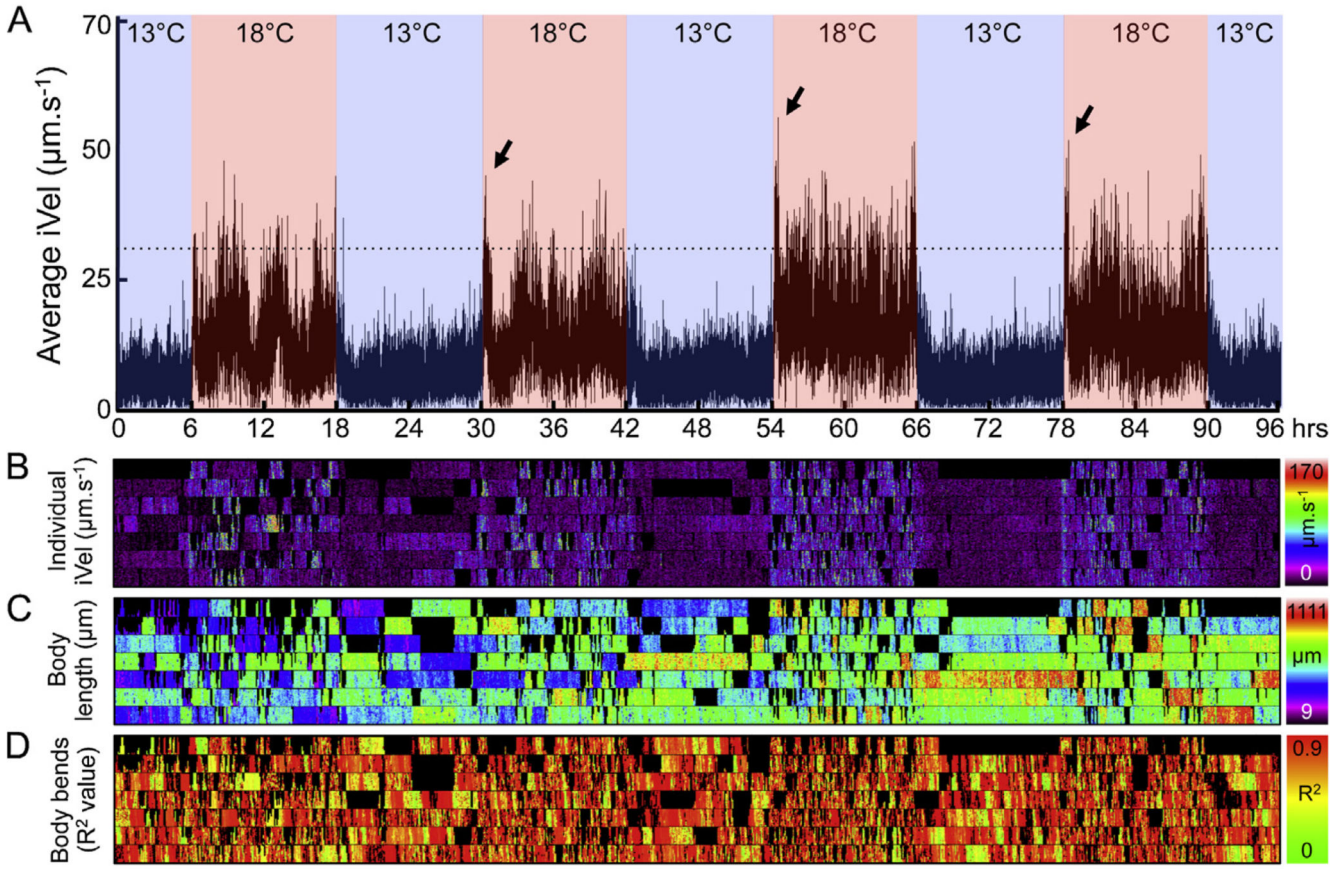

Fig. 3.

Locomotor activity rhythms and features related to movement and shape in wild-type animals during temperature cycles. (A) A line graph showing the average instantaneous velocity (iVel) of successfully tracked animal population ($n = 7$) during 4 days of temperature cycles of 13 °C:18 °C (12:12 h). The warm (18 °C) and cold (13 °C) phase of the cycle are depicted by red and blue colors, respectively. Sudden bursts in activity (startle response) are indicated with black arrows. Spatio-temporal maps of iVel (µm s^{-1}) (B), body length (µm) (C), and the R^2 value for linearity (degree of body bends) (D) of individual animals successfully tracked for about 30 s are shown. (For interpretation of the references to color in this figure legend, the reader is referred to the web version of this article.)

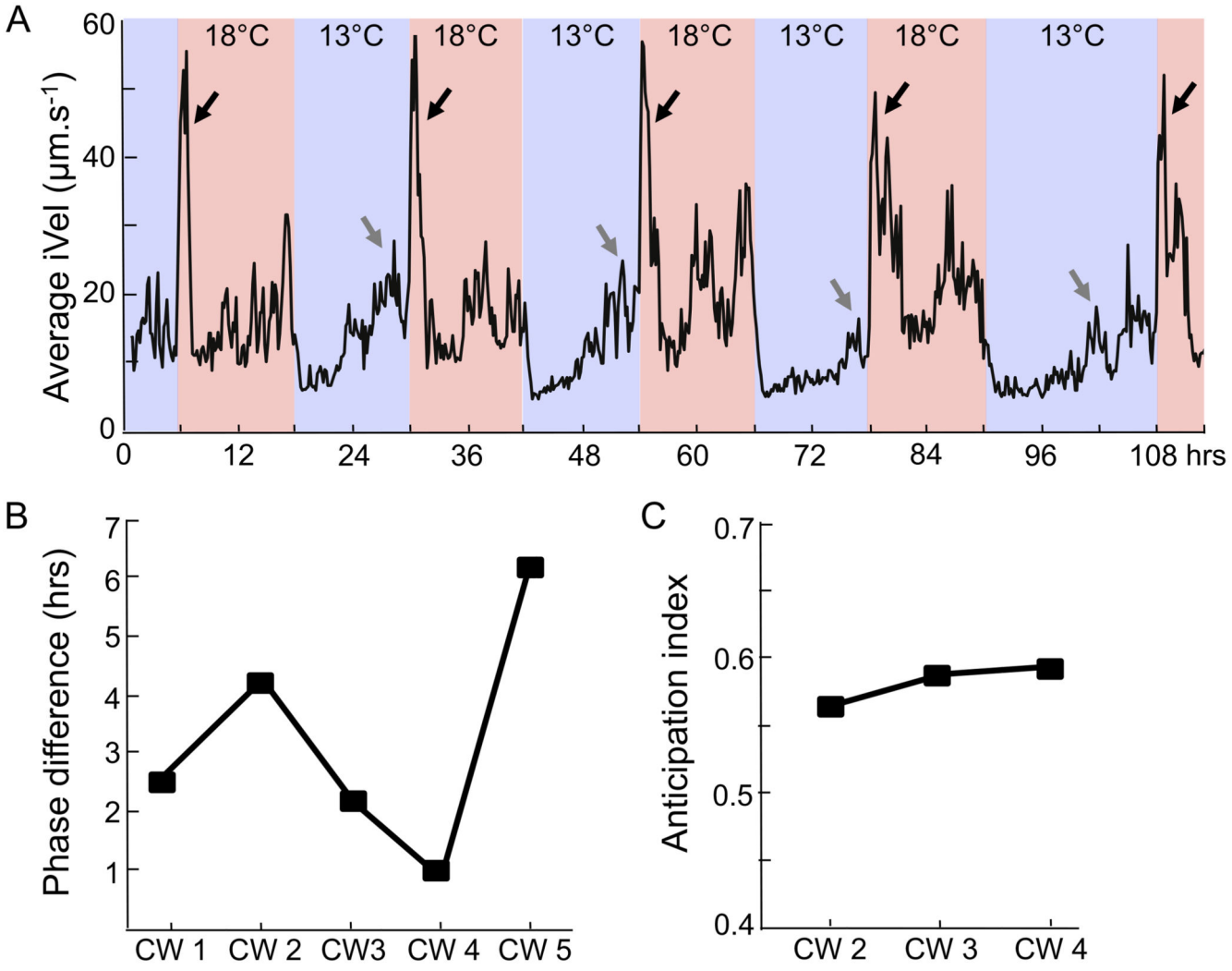

Fig. 4.

Anticipatory behavior of the wild-type animal population. (A) A line graph showing average instantaneous velocity (iVel) of successfully tracked population of wild-type animals ($n = 7$) binned in 10 minute-average intervals during 4 days of 13 °C:18 °C (12:12 h) temperature cycles (CW 1–4) and a fifth day (CW 5) in which the warm phase is delayed by 6 h (13 °C: 18 °C, 18:6 h). Anticipatory increase in activity levels, and sudden bursts in activity (startle response) are indicated with gray and black arrows, respectively. Animals were placed on FUDR plates at the L4 stage as opposed to young adults (see Section 2). The warm (18 °C) and cold (13 °C) phase of the temperature cycle are depicted by red and blue colors, respectively. (B) Quantification of the phase differences between the timing of increased activity onset and start of the warm (18 °C) phase of the temperature cycle (expressed in hours) for each cold-warm (CW) day (see Section 2). (C) Quantification of anticipation indices for days CW 2–4. Anticipation indices to the warm (18 °C) phase are expressed as the fraction of total activity during the last 3 h of the cold (13 °C) phase to total activity during the 6 h preceding the warm (18 °C) phase. Higher values (>0.5) indicate greater

anticipation. (For interpretation of the references to color in this figure legend, the reader is referred to the web version of this article.)

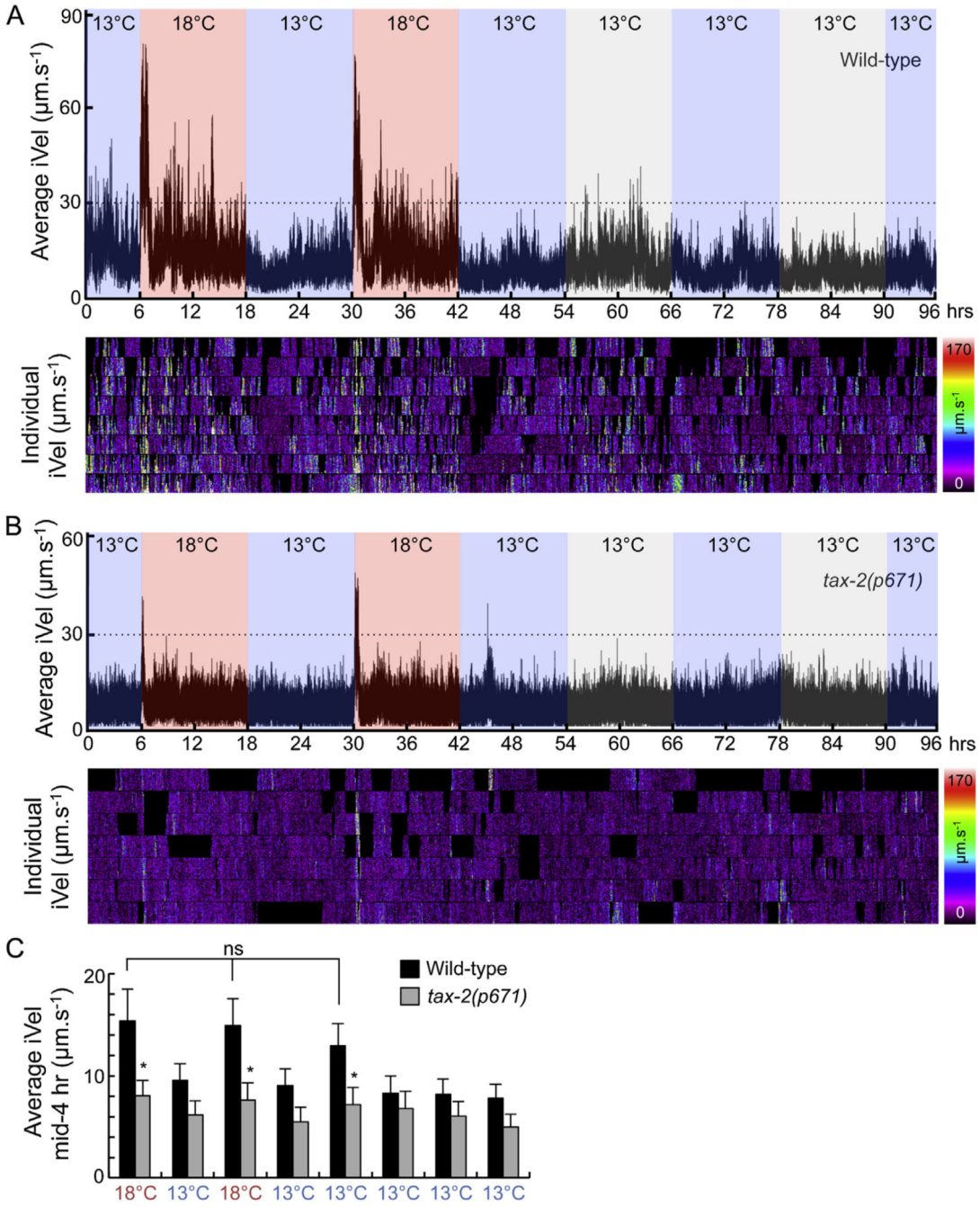

Fig. 5.

Rhythms in locomotor activity of wild-type and *tax-2* mutant animals during temperature entrainment and free-running. A line graph showing the average instantaneous velocity (iVel) of a successfully tracked population of wild-type animals ($n = 7$) (A) and *tax-2(p671)* mutant animals ($n = 7$) (B) as a measure of locomotor activity in µm s^{-1} during 2 days of temperature (13 °C:18 °C) entrainment, followed by 2 days of free-running at 13 °C. Spatio-temporal maps of iVel (µm s^{-1}) of individual animals successfully tracked for about 30 s are shown below each line graph. (C) The average iVel during the mid-4 h of each 12-h phase

for a population of wild-type and *tax-2(p671)* mutant animals. * indicates values that are different from that of wild-type at $P < 0.01$ using a two-way ANOVA. n.s. indicates the values between brackets that are not significantly different. Error bars denote the SEM. The warm (18 °C) and cold (13 °C) phase of the temperature cycle are depicted by red and blue colors, respectively, with the subjective warm phase depicted in gray colors. (For interpretation of the references to color in this figure legend, the reader is referred to the web version of this article.)